General Expression for the Voigt Function that is of Special Interest for Applied Spectroscopy

H. O. Di ROCCO, D. I. IRIARTE, and J. POMARICO*

Instituto de Fisica Arroyo Seco, Facultad de Ciencias Exactas, Universidad Nacional del Centro, Pinto 399, 7000 Tandil, Argentina

The purpose of this work is twofold. First we obtain a series expansion for the Voigt function that is valid for all values of the dimensionless parameter *a* (a measure of the ratio between the Lorentzian and Gaussian widths). Furthermore, the resulting coefficients are independent of the generalized coordinate *b* (the wavelength measured in units of the Gaussian width). In the second place, we fit an experimental "shaped bell" curve to a Voigt profile using certain theoretical restrictions that relate the maximum height and the full width at half-maximum.

Index Headings: **Spectroscopy; Profile; Voigt function.**

INTRODUCTION

Line shapes provide fundamental information in applied spectroscopy, since transition probabilities, electron and ion temperatures, and electron densities are related to them in different ways. The Voigt profile, $V(x)$, defined as the convolution between a Gaussian and a Lorentzian function [denoted $G(x)$ and $L(x)$, respectively], is useful in the physics of stellar atmospheres and in optical spectroscopy, where a thermal distribution of velocities (a Gaussian) must be folded with the function describing the broadening of spectral lines by electron collisions (a Lorentzian). The Voigt profile has been treated from the graphical and numerical point of view. Calculations and graphs were given, for example, by van de Hulst and Reesnick.[1] An approximation to the standardized Voigt function was made by Kielkopf[2] and a computational procedure was published by Drayson.[3] Classic papers on the subject are contained in these last two references. Recent publications summarizing diverse types of approximations are due to Thompson[4] and Brablec et al.[5]

Many works were made by astrophysicists; their main interest involves the case where the Gaussian width is more important than the Lorentzian one. This relation is taken into account with respect to the so-called *a* parameter, the ratio between Lorentzian and Gaussian widths (see Eq. 10 below), which, for this case, is <1. Several series and asymptotic expansions can be found in the above-cited papers and in the classic books by Unsold[6] and Mihalas.[7] On the other hand, when $a > 1$, the only known expression is due to Traving[8] and is restricted to the case $a > 1.4$.

The present work consists of two main parts: (1) The development of a new expression for the Voigt function that is valid for all values of the parameter a. This expression is of particular interest when $a > 1$ because of its applicability in the spectroscopy of cold and dense plasmas. (2) The fitting of experimental points to a Voigt profile, based on theoretical properties (or restrictions) of the operations *height times width* and *height divided by width*. To this end, we propose a criterion based on the peak value of the profile and on its full width at half-maximum (FWHM). This feature is important because, in this region, around the peak, the signal-to-noise ratio is better than in the wings.

In terms of applications, we consider some important uses of the Voigt function in the practical analysis of the experimental profiles: (1) the discrimination of the bound–bound transition with respect to the continuum, and (2) the estimation of the total line intensities, defined as $I = \int_{-\infty}^{\infty} I_\lambda \, d\lambda$ where, in practice, the line wings are cut off relatively close to the line center at distances only a few times the half-width. Both questions are, of course, closely related. Furthermore, in spectroscopy of cold dense plasmas (when the electron density $N_e \approx 10^{16}$–10^{18} cm^{-3}, the electron temperature T_e reaches some eV, and $T_e \geq T_i$, the ion temperature), the basic problem is the determination of the plasma broadening width and the ion temperature, knowing that both the ion contribution to the broadening and the instrumental function can be treated as Gaussian functions. This factor is useful for applications where transition probabilities must be obtained and also for studies of the physics of electric discharges and laser-produced plasmas (LPPs). All these applications are of direct interest for laser-induced breakdown spectroscopy (LIBS).[9] In fact, when the plasma source can be regarded as thin, line intensities are proportional to the transition probabilities, and electron temperature and densities are needed in the calculation of Saha and Boltzmann distributions.

In the next section, we present a concise revision of the notations and definitions and, in the following section, an exact expression for the Voigt function. The fourth section is devoted to the description and test of an algorithm proposed for deconvolution of a Voigt profile into its Gaussian and Lorentzian components. Finally, the main conclusions of this work are summarized.

THE VOIGT PROFILE

There is a wide and confusing variety of notations for the Voigt profile. Therefore, in this section, we present a brief discussion of this point. To this end, the normalized expressions for the distributions (those making the area under the curves equal to unity), $G(x)$ and $L(x)$, will be used. The argument x may denote frequency or wavelength. The corresponding FWHMs (Γ_G and Γ_L) will be introduced to define the operations "height times width" and "height divided by width" for both types of curves, since they are very useful when experimental points are to be fitted to a Voigt profile. The following notation will be used: ω for the parameters giving the simplest nor-

Received 10 November 2000; accepted 14 March 2001.

* Author to whom correspondence should be sent.

0003-7028/01/5507-0822$2.00/0

malized expression, Γ for the FWHM, and γ for the half-width at half-maximum (HWHM); lower indexes *G, L,* and *V* indicates Gauss, Lorentz, and Voigt, respectively.

Gaussian Profile. In this case, $G(x)$ is written as

$$G(x) = G_0 \exp[-(x/\omega_G)^2] \tag{1}$$

where ω_G, the Gaussian parameter, is related to the Gaussian HWHM (γ_G) through

$$\omega_G = \frac{\gamma_G}{\sqrt{\ln 2}} \quad \text{and} \quad G_0 = \frac{1}{\sqrt{\pi}\omega_G} \tag{2}$$

For this normalized curve the product of the maximum height times the FWHM is

$$G_0 \times \Gamma_G = 2\sqrt{\ln 2/\pi} \approx 0.93944 \tag{3}$$

whereas the ''svelteness'', the ratio between the maximum height and the FWHM, is

$$\frac{G_0}{\Gamma_G} = \frac{2\sqrt{\ln 2/\pi}}{\Gamma_G^2} \approx \frac{0.93944}{\Gamma_G^2} \tag{4}$$

Lorentzian Profile. Analogous to the previous case,

$$L(x) = L_0 \frac{\omega_L^2}{(x^2 + \omega_L^2)} \tag{5}$$

where ω_L is the Lorentz parameter related to the Lorentz HWHM through $\omega_L = \gamma_L$ and

$$L_0 = \frac{1}{\pi\omega_L} \tag{6}$$

Now

$$L_0 \times \Gamma_L = 2/\pi \approx 0.63662 \tag{7}$$

and

$$\frac{L_0}{\Gamma_L} = \frac{2}{\pi\Gamma_L^2} \approx \frac{0.63662}{\Gamma_L^2} \tag{8}$$

The Voigt Profile. From Eqs. 1 and 5, the convolution between both functions is given by

$$V(x) = \frac{(\omega_L/\omega_G)}{\pi^{3/2}} \int_{-\infty}^{\infty} \frac{e^{-(x'/\omega_G)^2}}{(x - x')^2 + \omega_L^2} \, dx' \tag{9}$$

with the normalization condition

$$\int_{-\infty}^{\infty} V(x) \, dx = 1$$

Defining the dimensionless parameters

$$y = x'/\omega_G;\ b = x/\omega_G;\ a = \omega_L/\omega_G \equiv \sqrt{\ln 2}\Gamma_L/\Gamma_G \tag{10}$$

the integral in Eq. 9 can be written as

$$V_a(b) = \frac{a}{\pi^{3/2}\omega_G} \int_{-\infty}^{\infty} \frac{e^{-y^2} \, dy}{(y - b)^2 + a^2} \tag{11}$$

which is the expression for the dimensionless function commonly appearing in the literature[6,7]. An equivalent result is obtained after making $u = (y - b)/a$; then

$$V_a(b) = \frac{1}{\pi^{3/2}\omega_G} \int_{-\infty}^{\infty} \frac{e^{-(au+b)^2} \, du}{u^2 + 1} \tag{12}$$

In Eqs. 11 and 12, the value of the integral is

$$\int_{-\infty}^{\infty} V_a(b) \, db = \frac{1}{\omega_G}$$

Therefore, in the following paragraphs, it will be useful to consider the Voigt dimension-less function $U_a(b)$ normalized to unity:

$$U_a(b) \equiv \omega_G V_a(b) \tag{13}$$

Taking into account that $1/(u^2 + 1)$ is the Laplace transform of $\cos(ux)$, we can write for $U_a(b)$ the equivalent expression

$$U_a(b) = \frac{1}{\pi a} \int_0^{\infty} e^{-x} e^{-(x/2a)^2} \cos(bx/a) \, dx \tag{14}$$

The peak intensity (when $b = 0$) is given in terms of the complementary error function $(1 - \text{erf}(a))$:

$$V_a(0) = \frac{e^{a^2}(1 - \text{erf}(a))}{\sqrt{\pi}\omega_G} \tag{15}$$

or, equivalently,

$$V_a(0) = \frac{ae^{a^2}(1 - \text{erf}(a))}{\sqrt{\pi}\omega_L} \tag{16}$$

Series and asymptotic expansions for $(1 - \text{erf}(a))$ can be found for both $a \leq 1$ and $a > 1$ in manuals on special functions.[10]

The FWHM of the Voigt Function and the Calculation of *a* from the Experimental Data. In the published literature we have not found a simple characterization of the Voigt FWHM from a neat theoretical analysis. Kielkopf[2] cites the graphs given by van de Hulst and Reesnik in order to arrive at an approximate solution of the problem, whereas Allen[11] gives an estimation for Γ_V without indicating the source. The Voigt FWHM depends on the parameters a and b defined in Eq. 10. For each a value, we call $b_{1/2}(a)$ the value of b such that $V_a(b_{1/2})/\omega_G = V_a(0)/2\omega_G$. This value of b is the HWHM in units of $\omega_G = \Gamma_G/2\sqrt{\ln 2}$. From Eq. 10 it holds that

$$b_{1/2}(a) = a\frac{\Gamma_V}{\Gamma_L} = \sqrt{\ln 2}\frac{\Gamma_V}{\Gamma_G} \tag{17}$$

This equation determines Γ_L once $b_{1/2}(a)$, a, and Γ_V are available. Then, Γ_G can be calculated. Moreover, from Eqs. 15, 16, and 17

$$V_a(0) \times \Gamma_V = \frac{2b_{1/2}(a)e^{a^2}(1 - \text{erf}(a))}{\sqrt{\pi}} \tag{18}$$

Equation 18 is exact, even when $b_{1/2}(a)$ is obtained numerically and with very good accuracy ($r^2 = 1$) from

$$b_{1/2}(a) = a + \sqrt{\ln 2}\exp[-0.6055a + 0.0718a^2 - 0.0049a^3 + 0.000136a^4] \tag{19}$$

For $a \ll 1$; $\Gamma_V \approx \Gamma_G$, whereas for $a \gg 1$, $\Gamma_V \approx \Gamma_L$. This is a very important result since it allows us, once $V_a(0)$ and Γ_V are known from the experimental data, to find the value of the parameter a and, therefore, Γ_L and Γ_G, thus leading to the deconvolution of the Voigt profile.

AN EXPANSION VALID FOR ALL VALUES OF *a*

Because much previous work was done by astrophysicists, all known expressions are for the case $a \ll 1$ where

the Gaussian term is dominant. We present here a general result that is valid for all values of the parameter a, thus also including the case $a > 1$, which is of special interest for the spectroscopy of cold and dense plasmas and LIBS applications.

From Eq. 14, using the representation

$$\cos\left(\frac{bx}{a}\right) = \sum_{n=0}^{\infty} \frac{(-1)^n}{(2n)!}\left(\frac{b}{a}\right)^{2n} x^{2n}$$

we can write

$$U_a(b) = \frac{1}{\pi a} \sum_{n=0}^{\infty} \frac{(-1)^n}{(2n)!}\left(\frac{b}{a}\right)^{2n} I_n \tag{20}$$

with

$$I_n = \int_0^{\infty} e^{-x} e^{-(x/2a)^2} x^{2n}\, \mathrm{d}x \tag{21}$$

From Ref. 10 and with the introduction of the parabolic cylinder functions $D_p(z)$

$$I_n = (1/2a^2)^{-2(n+1)/2}\Gamma(2n + 1)e^{a^2/2}D_{-(2n+1)}(\sqrt{2}a) \tag{22}$$

related to the confluent hypergeometric functions

$$M(\alpha, \gamma; x) = 1 + \frac{\alpha}{\gamma}\frac{x}{1!} + \frac{\alpha(\alpha + 1)}{\gamma(\gamma + 1)}\frac{x^2}{2!} + \cdots \tag{23}$$

through

$$D_{-(2n+1)}(\sqrt{2}a) = 2^{-(2n+1)/2}e^{-a^2/2}\left\{\frac{\sqrt{\pi}}{\Gamma(n + 1)}M\left(\frac{2n + 1}{2}, \frac{1}{2}; a^2\right) - \frac{2\sqrt{\pi}a}{\Gamma\left(\frac{2n + 1}{2}\right)}M\left(n + 1, \frac{3}{2}; a^2\right)\right\} \tag{24}$$

such that

$$U_a(b) = \frac{1}{\sqrt{\pi}} \sum_{n=0}^{\infty} (-1)^n \times \left\{\frac{1}{\Gamma(n + 1)}M\left(\frac{2n + 1}{2}, \frac{1}{2}; a^2\right) - \frac{2a}{\Gamma\left(\frac{2n + 1}{2}\right)}M\left(n + 1, \frac{3}{2}; a^2\right)\right\} b^{2n} \tag{25}$$

which, taking into account Eqs. 13 and 17, results in

$$V_a(x) = \frac{b_{1/2}}{\sqrt{\pi}\gamma_V} \sum (-1)^n \left(\frac{b_{1/2}}{\gamma_V}\right)^{2n} v_n x^{2n} \tag{26}$$

v_n being the expression in brackets in Eq. 25.

It is very remarkable that the coefficients do not depend on b. This is not so for the case $a < 1$ presented in the literature,[6,7] where all coefficients depend on both the summation index n and the ordinate b. This evaluation is simplified by the existence of recursion relations concerning the M functions.[10]

For $a = 0$, $M(\alpha, \gamma; a^2) = 1$, and we get the expansion for $G(x)$. For $a \to \infty$, using the asymptotic expansion for $M(\alpha, \gamma; x)$

$$M(\alpha, \gamma; z) \sim \frac{\Gamma(\gamma)}{\Gamma(\gamma - \alpha)}(-z)^{-\alpha}G(\alpha, \alpha - \gamma + 1; -z) + \frac{\Gamma(\gamma)}{\Gamma(\alpha)}e^z(z)^{\alpha-\gamma}G(\gamma - \alpha, 1 - \alpha; z) \tag{27}$$

v_n is

$$v_n = \frac{(-1)^{-(n+1)}\sqrt{\pi}}{\Gamma\left(\frac{2n + 1}{2}\right)\Gamma\left(\frac{1 - 2n}{2}\right)a^{2n+1}}$$

and taking into account that

$$\frac{1}{\Gamma\left(\frac{2n + 1}{2}\right)\Gamma\left(\frac{1 - 2n}{2}\right)} = \frac{(-1)^n}{\pi}$$

and $b/a = x/\omega_L$, we have

$$U_{a\to\infty}(b) = \frac{\omega_G}{\pi\omega_L} \sum_{n=0}^{\infty} (-1)^n \left(\frac{x}{\omega_L}\right)^{2n}$$

such that, from Eq. 13

$$V_{a\to\infty}(x) = \frac{1}{\pi\omega_L} \sum_{n=0}^{\infty} (-1)^n \left(\frac{x}{\omega_L}\right)^{2n}$$

which is the expansion of $L(x)$.

ALGORITHM FOR PROFILE DECONVOLUTION

As stated above, Eq. 18 allows us to find the Lorentzian and Gaussian widths of the Voigt profile in terms of the parameter a, provided that the peak value $[V_a(0)]$ and the experimental Voigt FWHM (Γ_V) are known. Moreover, from Eqs. 3 and 7 it is clear that if a set of "shaped bell" experimental points is expected to be well fitted by a Voigt curve, then the product of the maximum experimental height times the experimental FWHM must be between 0.939 and 0.636, whereas the svelteness must be between the values given by Eqs. 4 and 8. In the rest of this section we describe how $V_a(0)$, Γ_V, and also the parameter a can be obtained from the experimental data, which are usually affected by noise.

The algorithm goes through the following main steps:

(1) The absolute intensity maximum (I_{MAX}) of the experimental points and its corresponding position, λ_{MAX} and P_{MAX}, in wavelength and pixels units, respectively, are found. Due to the discrete nature of the data, I_{MAX} does not necessarily occur at the actual center wavelength of the observed line. When noise is not very important and the data points are sufficiently spaced, a parabolic interpolation can be used to introduce a correction to I_{MAX} to find the actual peak intensity $V_a(0)$. On the other hand, when many data points are available, integration under the profile can be used to this end.

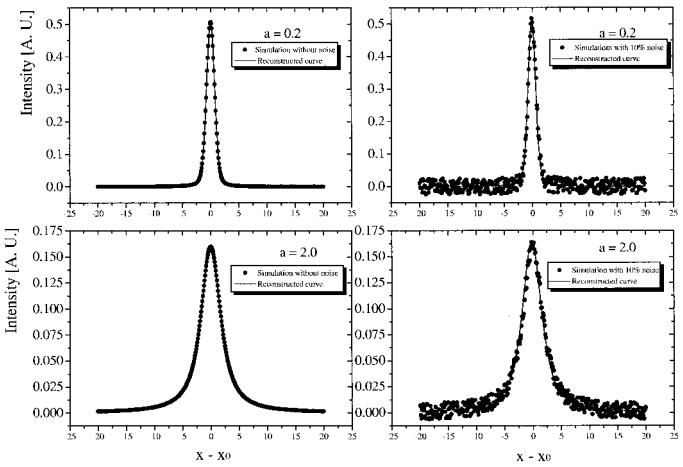

FIG. 1. Simulated data (scatter points) and their corresponding reconstructed profiles (solid lines) for two different values of the parameter a and for different noise levels.

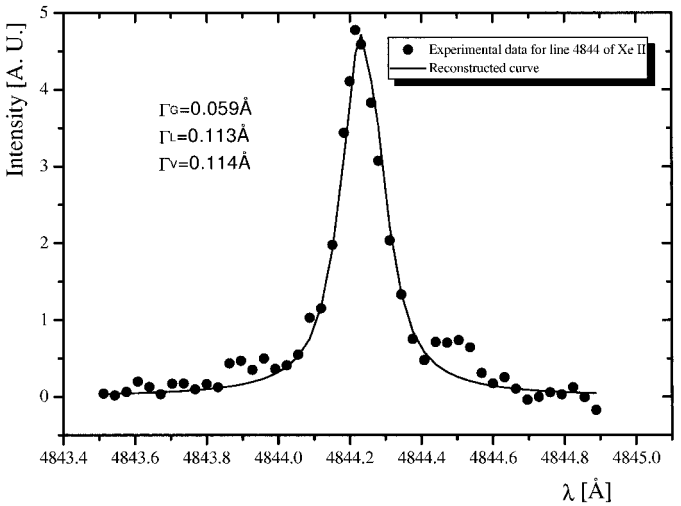

FIG. 2. Experimental data points (scatter graph) corresponding to the line 4844 Å of Xe(II) and the Voigt profile obtained after applying the algorithm (solid line).

(2) As a first approach to obtaining FWHM, two pixels are found (one to the left and one to the right of P_{MAX}) for which the difference between their corresponding intensity values and $V_a(0)/2$ is a minimum. An interpolation is then used at both sides to find the points giving exactly half the value of $V_a(0)$. The distance between these points (in wavelength units) is the desired FWHM, Γ_V.

(3) The product $V_a(0) \times \Gamma_V$ is evaluated and compared to the right-hand term of Eq. 18. This is done by computing this term for different values of the parameter a, which is moved in small steps until a desired degree of accordance is achieved. As seen from Eq. 18 and discussed in the preceding section, the limit $a = 0$ represents a pure Gaussian profile, while the limit $a \rightarrow \infty$ corresponds to a pure Lorentzian curve. However, in practice, the variation of the parameter a can be confined between 0 and 5, since for values of a greater than 5 the right-hand term of Eq. 18 differs from its limit value $2/\pi$ in less than 1% and the profile can be considered as pure Lorentzian, as is shown below.

With this known value of a, the Lorentzian and Gaussian FWHMs, Γ_L, and Γ_G, respectively, are evaluated, and the entire profile can be reconstructed and compared with the actual one in terms of a merit figure such as χ^2.

Test of the Algorithm. To verify the above described procedure for profile deconvolution, we numerically generated Voigt profiles from the exact convolution integral defined in Eq. 11 and for different values of a. In that procedure, the Gauss FWHM (Γ_G) was fixed at 1.5 and, for the different values of a, the Lorentz FWHM was obtained accordingly with Eq. 10. White noise was also added to these profiles to simulate laboratory conditions. Figure 1 presents the results for Voigt profiles constructed with $a = 0.2$ and $a = 2$ (scatter graphs) together with the corresponding reconstructed profiles (solid lines).

The algorithm was then applied to a set of experimental data corresponding to the line of 4844 Å of Xe(II) to test its performance under real laboratory conditions. Spectral lines were measured from an LPP excited by focusing a 400 mJ Nd:YAG laser delivering 7 ns pulses at 1.06 μm onto a cell containing Xe at 300 mTorr. The scanning of the observed lines was carried out by a shot-by-shot technique, rotating in small steps (0.05 Å min^{-1}) the grating of a monochromator with a resolving power of 300 000 and using a photomultiplier (PM) as detector. The signal from the PM was processed by a boxcar averager and recorded as a sequential file after proper digitalization. Each recorded data point was the result of an average over (typically) 30 laser shots to improve the signal-to-noise ratio. The number of recorded data can be varied, 60 points being a good compromise between resolution and scanning time. Figure 2 shows both the experimental data points (scatter graph) and the Voigt profile (solid line) obtained after applying the algorithm. For this profile, the algorithm gives $\Gamma_G = 0.059$ Å and $\Gamma_L = 0.113$ Å.

The obtained Gaussian width is itself the convolution of two Gaussian contributions—namely, the Doppler broadening of the line, directly related to the ion temperature of the plasma, and the monochromator slit. Moreover, the instrumental function of a monochromator when both the entrance and exit slit are equal is theoretically a triangle function $[T(x)]$, which in certain cases can be very well approximated by a Gaussian profile. Indeed, numerical calculations presented in the book by Zaidel et al.[12] indicate the similarity between the convolutions $L(x) * G(x)$ and $L(x) * T(x)$ for such slits.

The convolution of two Gaussians is also a Gaussian of total width following the equation $\Gamma_G^2 = \Gamma_{Doppler}^2 + \Gamma_{slit}^2$. Taking into account that the spatial resolution while registering the experimental line was set to 1 Å/mm and that both the entrance and exit monochromator slits were fixed at 30 μm (thus corresponding to a width of 0.03 Å), the resulting Gaussian width due to the Doppler effect is

$$\Gamma_{Doppler} = \sqrt{\Gamma_{Doppler}^2 - \Gamma_{Slit}^2} = 0.05 \text{ Å},$$

giving an ion temperature of 2.4 eV.[13]

Miscellaneous. We present here some numerical results which can be useful to fix orders of magnitude for the intervals of interest for the parameter a while running the code which implements the algorithm described above.

The expression

$$ae^{a^2}(1 - \text{erf}(a))$$

has a limit value (for $a \to \infty$) of $1/\sqrt{\pi}$. On the other hand, as can be seen from Eq. 19, for $a > 1$, $b_{1/2}(a)$ tends rapidly to a. Thus as a becomes greater, the numerator of Eq. 18 can be replaced by its limit value with an error that is negligible for $a = 5$ and up. In fact, if $a = 4.5$, the expression

$$\frac{ae^{a^2}(1 - \mathrm{erf}(a))}{\sqrt{\pi}}$$

comes to 0.31632. Thus, the entire expression can be replaced by its limiting value, $1/\pi = 0.31831$, representing an error of less than 1%.

In practice this means that if the noise present in the experimental data is greater than 1% (a value which is very easy to attain), a value of $a \geq 4.5$ makes the difference between $L(x)$ and $V(x)$ nonsense, and they can be considered indistinguishable.

If the noise is 10% or greater, the same arguments apply for $a \geq 2$.

These conclusions were taken into account when limiting the range of a to a maximum value of 5 in the program code of the algorithm described above.

CONCLUSION

We obtained a series expansion for the Voigt function $V(x)$ that is valid for all values of the parameter a (Eqs. 25 and 26). A concise relation between the peak value of the Voigt function and its FWHM was also derived (Eq. 18). This approach allows for an easy fitting of experimental points to a Voigt profile, using these analytic properties.

Additionally, a simple algorithm for profile deconvolution was developed and tested with the use of both simulated and actual experimental points. Results show very good agreement, as can be seen in Figs. 1 and 2, respectively. We emphasize the use of the peak value and the FWHM, because in this region the signal-to-noise ratio is better than in the wings.

1. H. C. van de Hulst and J. J. M. Reesnick, Astrophys. J. **106,** 121 (1947).
2. J. F. Kielkopf, J.O.S.A. **63,** 987 (1973), and references therein.
3. S. R. Drayson, J. Quant. Spectrosc. Radiat. Transfer **16,** 611 (1976).
4. W. J. Thompson, Computers Phys. **7,** 627 (1993), and references therein.
5. A. Brablec, D. Trunec, and F. Stastny, J. Phys. D **32,** 1870 (1999).
6. A. Unsold, *Physik der Sternatmospharen* (Springer, Berlin, 1968), and references therein.
7. D. Mihalas, *Stellar Atmospheres* (W. H. Freeman, San Francisco, 1978), pp. 279–281 and references therein.
8. G. Traving, "Line Broadening and Line Shift", in *Plasma Diagnostic,* W. Lochte-Holtgreven, Ed. (North Holland, New York, 1968).
9. *Laser Induced Plasmas and Applications,* L. J. Radziemski and D. A. Cremers, Eds. (Marcel Dekker, New York, 1989).
10. I. S. Gradshteyn and I. M. Ryzhik, *Tables of Integrals, Series and Products* (Academic Press, San Diego, California, 1980).
11. C. W. Allen, *Astrophysical Quantities* (Athlone Press, London, 1975), 3rd ed., p. 85.
12. A. N. Zaidel, G. V. Ostrovskaya, and Yu. I. Ostrovski, *Técnica y Práctica de Espectroscopia* (Ed. Mir, Moscú, 1979), pp. 19–32.
13. I. I. Sobelman, L. A. Vainshtein, and E. A. Yukov, *Excitation of Atoms and Broadening of Spectral Lines* (Springer, Berlin, 1981).